Nanomagnetism

DOI: 10.1002/anie.201105428

Exploring the No-Man's Land between Molecular Nanomagnets and Magnetic Nanoparticles

Dante Gatteschi, Maria Fittipaldi, Claudio Sangregorio, and Lorenzo Sorace*

cluster compounds · EPR spectroscopy · iron · magnetic properties · nanoparticles

The comparison of the structural and magnetic properties of molecular nanomagnets (MNM) and magnetic nanoparticles (MNP) can be instructive to get a deeper understanding of the magnetic behavior on the intermediate scale between molecular and bulk objects. In this respect iron oxo based clusters are particularly interesting, since they provide an increasing number of molecular systems with sizes close to that of iron oxide MNP. In this Minireview we report a survey of literature data aimed at improving our understanding of the emergence of MNP properties from MNM ones.

1. Introduction

Iron oxides are perhaps among the first functional materials used by humans, taking advantage of their color and of their magnetic properties. Even after a few millennia they are still of much interest, the nano revolution having provided new opportunities of investigation. In fact nanosized magnetic iron oxides have new properties which are exploited in such different areas as nanomedicine and information technology.[1] There is now a continuous transition from micro to nanoparticles which allows for the separate investigation of different size ranges and consequently different properties. Particles larger than 10 nm (corresponding to more than 10^5 iron ions) are usually considered as small parts of oxides and their magnetic properties interpreted using a top-down approach. On the other hand, when particles in the range of 1–5 nm, comprising 10–10000 ions, are investigated, a molecular bottom-up approach may be more useful. This size range is also particularly promising for observing new properties associated with the co-existence of classical and quantum behaviors.[2–5] In fact the explosive development of molecular nanomagnetism in the last few years has been ignited by the discovery that some molecules can behave as single molecule magnets (SMM), that is, show a blocked magnetization at low temperature and give stepped magnetic hysteresis.[6,7] The stepped magnetic hysteresis is the proof of the coexistence of quantum and classical effects. This breakthrough started a hunt to SMM with "improved" properties which produced some new molecules showing slow relaxation of the magnetization, and a large number of clusters which do not. All these complexes, referred to as molecular nanomagnets (MNM)[8] offer however the opportunity to understand the transition between the behavior of a single paramagnetic center and that of a cluster of n ions, with n increasing to very large values. A related active field is that of large iron oxo clusters, the study of which was initially prompted by the search for models of the growth of natural oxo hydroxides and of iron biomineralization.[9–11] Appealing as it can be, the molecular approach has been able to produce iron oxo based MNM with $n = 30$ as a maximum. The next step would be that of $n = 100$–1000, which currently is better covered by magnetic nanoparticles (MNP). Therefore efforts must be made to synthesize clusters with large and controlled values of n and emerging properties sought.[12] The goal of this Minireview is indicating to a general audience what has been circulating in the specialized literature, reporting the current understanding of the correlation between structural and magnetic properties of MNP of 1–5 nm, and comparing these properties with those of iron oxo based molecules. We are not covering in detail all the reported iron oxo clusters, for which excellent Reviews are available[9a] but rather we focus on systems which can be considered as milestones in the ideal bottom-up approach, that is, molecular systems which for structure and/or magnetic properties describe the transition from isolated ions to MNP. The choice has been further limited to those clusters for which an extended magnetic characterization is available. On the other side, we will discuss some examples of small ($d < 4$ nm) MNP, looking for the possibility to observe quantum effects. In particular we will focus on MNP which can be grown using solution chemistry techniques or taking advantage of natural nanolaboratories as

[*] Prof. D. Gatteschi, Dr. M. Fittipaldi, Dr. L. Sorace
Department of Chemistry and RU INSTM, University of Florence
Via della Lastruccia 3, 50019 Sesto Fiorentino (FI) (Italy)
E-mail: dante.gatteschi@unifi.it
Homepage: http://www.unifi.it/lamm
Dr. C. Sangregorio
CNR ISTM, via C. Golgi 19, 20133 Milan (Italy)

those provided by oligomeric ferritin-like proteins such as Dps (DNA binding proteins from starved cells),[13] which have an inner cavity of about 4 nm diameter, hosting up to 600 ions. Under specific conditions, in both ferritin and Dps it is possible to synthesize uniform magnetite or maghemite cores.[14,15]

We will first briefly review some aspects of nanomagnetism which are common to both MNP and MNM: in particular we will stress the importance of defining the magnetic anisotropy and saturation magnetization in a way which allows direct and meaningful comparison between the properties of the two classes of materials. In the same Section we will discuss how the electron magnetic resonance (EMR) spectra depend on the size of the systems. We use the acronym EMR in place of EPR (electron paramagnetic resonance) to stress that the resonance experiments are not performed only on simple paramagnetic systems. This discussion is followed by an overview of the structure and magnetic properties of selected examples of iron oxo clusters, highlighting the properties which tend toward those of MNP (such as, the role of "surface" anisotropy, loss of fine structure in EMR spectra). The fourth Section is devoted to a short review of the smallest iron oxide MNP synthesized to date and to show how EMR can be a very useful tool to investigate the properties of such systems allowing the emergence of quantum behavior as the size of the MNP is reduced to be detected

2. Nanomagnetism: Basic Concepts

Isolated ions behave as paramagnets, that is, their magnetization fluctuates freely averaging to zero unless a magnetic field is applied. After the application and subsequent removal of an external field, the magnetization relaxes with a characteristic time τ. The relaxation depends on several different mechanisms, of which the Orbach process, associated with the presence of an excited level at energy Δ, is particularly important. The relaxation originates from the absorption and emission of phonons of energy close to Δ and the dynamics follows an Arrhenius law. Switching on an interaction between the ions imposes a correlation between the individual spins which eventually determines a collective behavior. When the number of correlated spins, N, becomes infinite the magnetization is blocked.

In a MNP, where N is large but not infinite, the single-domain state is the most favorable, that is, all the constituent spins move simultaneously and behave as a giant spin. The magnetization relaxes following an Arrhenius law with a barrier $\Delta = KV$, where V is the volume of the particle and K is a constant called the anisotropy energy density. If $k_B T$ is small compared to the energy barrier for the re-orientation, Δ, the magnetization is blocked while at high temperature the magnetization fluctuates as in a paramagnet and the particles are said to be in the superparamagnetic state (Scheme 1, left). The blocking temperature, T_B, is the temperature at which the relaxation time of the magnetization equals the time scale of the technique used for the measurement.[16]

A similar behavior (Scheme 1, right) is observed in SMM: in this case the system is characterized by a total spin S arising from the coupling between the single paramagnetic centers and the anisotropy is described by a parameter D ($D<0$ for easy axis anisotropy), which provides a barrier to the reorientation of the magnetization equals to $|D|S^2$ for integer S and $|D|(S^2-1/4)$ for half integer values of S. The peculiar magnetic behavior of MNMs and MNPs depends then on the magnetic anisotropy, the relation between the parameters accounting for it in MNM and MNP being $K = -\alpha D S^2$, where $\alpha = N_A\rho/MW$ (N_A = Avogadro's number, ρ =

Dante Gatteschi has been Professor of Chemistry at the University of Florence since 1980. His research interests, initially focused on the investigation of coordination compounds, have subsequently been largely centered on the development of molecular magnetism, an area in which he has been one of the pioneers.

Claudio Sangregorio graduated in Chemistry at the University of Florence and obtained the PhD in Materials Science at the same institution. At present he is a researcher at the ISTM institute of the Italian CNR. His interests are in the field of nanosized magnetic materials, including metal oxide based nanocomposites for biomedical applications (magnetic fluid hyperthermia and MRI), magneto-plasmonic active nanoheterostructures, and high-spin molecular clusters.

Maria Fittipaldi (PhD in Physics, Leiden) is a lecturer at the University of Florence, Department of Chemistry. Her research activity is mainly dedicated to the study of nanostructured magnetic materials. She also investigates biological and inorganic systems ranging from metallo- and hemeproteins to doped semiconductors in order to correlate the electronic structure with function and properties.

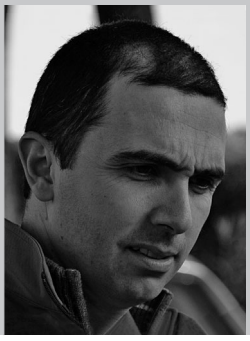

Lorenzo Sorace (PhD in Chemistry, Florence) is Lecturer at the University of Florence at the Chemistry Department. His main research interest is in the use of multifrequency EPR spectroscopy for the study of the magnetic anisotropy in molecular nanomagnets and rare-earth-based systems. More recently his interest has shifted towards the EPR characterization of nanostructured systems, ranging from surface deposited organic radicals to iron oxide based nanoparticles.

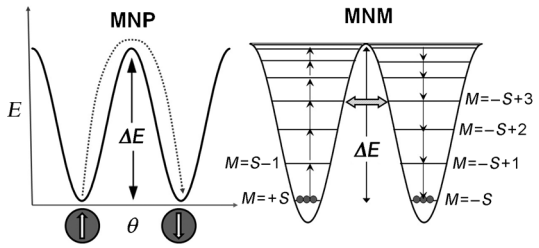

Scheme 1. The relationship between the barriers to the magnetization reorientation of MNP (left) and MNM (right).

sample density, MW = molecular weight). We stress that, to date, a systematic comparison between the two quantities has never been attempted. The magnetic anisotropy arises from several contributions: 1) single ion anisotropy, which depends on the geometry of the individual ions; 2) dipolar anisotropy, arising from the interaction between the ions; 3) shape anisotropy. For MNM, if the coupling scheme is known, both single ion and dipolar anisotropy terms can be calculated by summing each individual contribution weighted for a coefficient which depends on the spin state of the cluster. On the other hand, since for MNP the contribution of each individual ion cannot be determined, single ion anisotropy is subdivided in two different classes: 1) magnetocrystalline anisotropy, which refers to the anisotropy of the core of the MNP and is considered equal to the anisotropy of the corresponding bulk material; 2) surface anisotropy, arising from the low symmetry and coordination of the surface ions, which are particularly numerous in ultrasmall MNP. Finally, the shape anisotropy originates from the magnetostatic energy, which makes the sample more easily magnetized in the direction of its largest dimension. This term is usually not considered for MNM, although it may be shown that the spatial arrangement of magnetic ions is relevant in determining the global anisotropy of the system.[12]

Other important parameters to compare in the two classes of compounds are the saturation magnetization per iron atom and per volume unit, which provide information on the relative orientation of the individual spins and on their density in the investigated material. With the aim of developing a common ground for the discussion of the magnetic properties of these systems, the saturation magnetic moment and the anisotropy density were calculated from the data available in the literature and collected in Tables 1 and 2.[17]

The emergence of new properties in nanomagnets can be probed by EMR experiments.[12] At low temperature discrete transitions between the split components of the ground spin state S are observed. On increasing n the gap between the low-lying levels decreases and the quantum features vanish. Similar results are observed on increasing T. On the other hand the first signs of quantum effects in small MNP can be monitored by the observation of half-field resonances corresponding to $\Delta M = \pm 2$ transitions.[2,4]

3. Molecular Nanomagnets: Structures and Properties

3.1. Fe_8

The number of molecular iron oxo clusters is very large and a decision on the minimum number n of iron ions present in the molecule from which to begin a survey is largely arbitrary. We decided to start from $n = 8$, since a cluster of this nuclearity (**Fe_8Br**) was the second SMM discovered,[18] and was of fundamental importance for understanding the quantum effects in this class of compounds.[19] The structure of this cluster, reported by Wieghardt et al.,[20] is shown in Figure 1 a, indicating its planar character. The presence of many iron oxo triangles with competing antiferromagnetic interactions yields a ground $S = 10$ state.

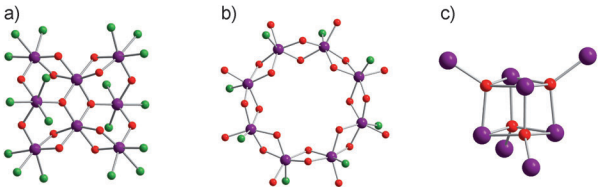

Figure 1. Different topologies of Fe_8 cores: a) frustrated planar structure, yielding $S = 10$, b) ring structure, providing $S = 0$ ground state, c) 3D oxide-like structure. Purple Fe, red O, green halogen.

The results of both EMR and inelastic neutron scattering provided evidence of a negative D value, corresponding to easy axis anisotropy[21] and were interpreted in the framework of the giant spin model,[22] showing a well resolved fine structure, indicating that the molecule behaves magnetically in a completely different way to MNP. The anisotropy density of the Fe_8 core is twice as large as that of the smallest reported maghemite MNP (Tables 1 and 2) but the corresponding anisotropy energy is ten times smaller, because the volume of the Fe_8 core is approximately 25-times smaller than that of the MNP.

Even at this relatively low n, different topologies and structures have been reported; although the interest so far has been mainly focused on clusters with a non-zero S ground state, systems with a ground state $S = 0$ can be interesting to monitor the transition between paramagnet and antiferromagnet on increasing the size of the cluster. Part of the family of the ferric wheels, originally synthesized by Lippard,[23] the octagonal rings[24] shown in Figure 1 b, can be considered as magnetic models for one-dimensional antiferromagnets. In fact the low-lying levels above the ground $S = 0$ state are accessible with several techniques. A detailed single crystal HF-EPR study has allowed the determination of the spin Hamiltonian parameters of the lowest multiplets with $S \leq 4$.[25] The data were also well reproduced by a dimer model of two sublattices of $S = 10$ with uniaxial anisotropy, allowing a very precise determination of both the exchange coupling and the single-ion contribution to the anisotropy, indicating that the physics of the systems is mainly determined by these terms of the spin Hamiltonian, with small effects of extra contributions.

Finally, the Fe_8 molecule shown in Figure 1c, where four Fe^{III} centers define a cubane bridged by four oxygen atoms to four external Fe^{III} ions can be considered as an analogue of a 3D structure. Indeed, it closely resembles the $Fe_8(\mu_4\text{-}O)_4$ unit present in all-ferric minerals, with Fe–O bond lengths within the range for the corresponding bonds of maghemite and ferrihydrite.[26] It is reported to have an $S=0$ ground state.

3.2. Iron Oxide-Like Clusters

Figure 2 shows the structures of some typical minerals to which molecular systems will be compared.

Lepidocrocite, α-FeOOH, is mimicked by the **Fe_{10}** cluster first described by one of us (Figure 3).[27] The core structure of parallel layers of Fe and O atoms and a cubic closest packing arrangement of the oxygen atoms is particularly stable and is found in several compounds with different external ligands.[28] The magnetic behavior of the **Fe_{10}** clusters is characterized by a ground state $S=0$, while no maximum in susceptibility is observed, suggesting spin frustration effects. Thus the presence of closely spaced spin states near the ground state, in other words, yields a solid-state-like behavior that is presumably related to the compact structure of the core. The situation is somewhat different for the similar system reported by Godbole et al.,[29] since field-dependent magnetization clearly shows the sign of a field-induced spin-state transition, suggesting a more discrete level structure.

Binding modes typical for hematite have been reported in a system containing an $Fe_{14}O_{12}(OH)_{16}$ core.[30] Magnetic studies pointed to the presence of an uncompensated magnetic moment arising from competing magnetic interactions, making the cluster similar to small antiferromagnetic MNP, such as those obtained from nanostructured hematite.[31]

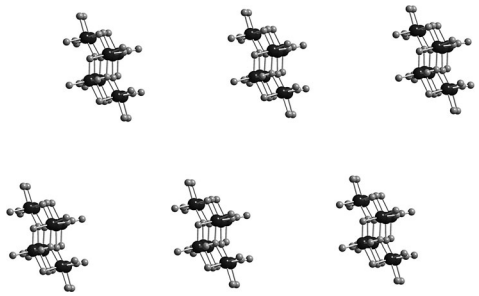

Figure 3. Packing of the lepidocrocite-like **Fe_{10}** cores.[27]

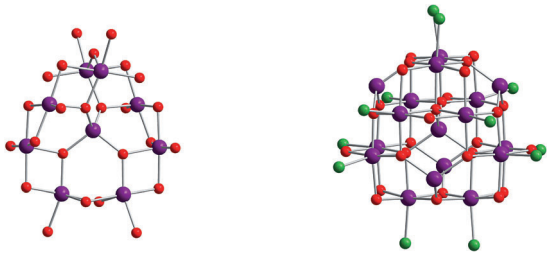

Figure 4. Cores of the magnetite like **Fe_9heia** (left) and **Fe_{17}py** (right) clusters reported in Ref. [32].

Fe_9 and Fe_{17} clusters resembling pieces of magnetite (**Fe_9heia** and **Fe_{17}py**) were reported by Evangelisti et al. (Figure 4).[32] Susceptibility data for both **Fe_9heia** and **Fe_{17}py** indicate the presence of antiferromagnetic interactions, with low-temperature maxima suggesting large spin ground states. For **Fe_9heia** the best fit was obtained for $S=25/2$, $g=1.99$, and $D=-0.07\ cm^{-1}$ while for **Fe_{17}py** magnetic data were initially fitted to an $S=35/2$ ground state with $D=+0.33\ cm^{-1}$;[32a] later measurements confirmed the ground-state value but suggested a weak easy-axis type anisotropy ($D<0$).[32b] More

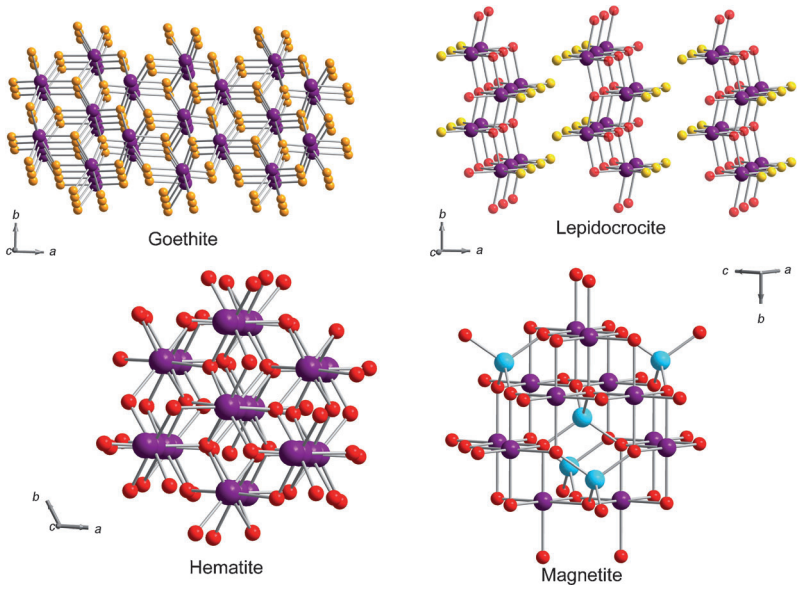

Figure 2. Structures of different Fe^{III} containing minerals. Purple octahedral iron centers, cyan tetrahedral iron centers, red oxygen, yellow hydroxy.

interestingly, the magnetic moment per volume unit obtained considering the volume of the inorganic core alone provides values which are close to those of bulk magnetite (see Table 1).

Mixed crystals of molecules containing $[Fe_{19}(\mu_3\text{-}O)_6(\mu_3\text{-}OH)_6(\mu_2\text{-}OH)_8]$, and $[Fe_{17}(\mu_3\text{-}O)_4(\mu_3\text{-}OH)_6(\mu_2\text{-}OH)_{10}]$ cores, hereafter **Fe_{19}heidi** and **Fe_{17}heidi**, capped by organic ligands and water molecules, were reported by Powell et al. (Figure 5).[33] The obtained clusters were colloquially termed by authors as "crusts" (standing for "cluster rust" or "captured rusts") to highlight their strong correlation to bulk iron oxyhydroxide phases. Both clusters can be regarded as composed by an inorganic core unit $[Fe_7(\mu_3\text{-}OH)_6(\mu_2\text{-}OH)_4\{\mu_3\text{-}O)Fe\}_2]^{3+}$ which can be recognized as a portion of a planar brucite type $\{Fe(OH)_2\}^+$ lattice enclosed in a cluster shell, comprising 10 (**Fe_{17}heidi**) or 12 (**Fe_{19}heidi**) peripheral Fe^{III} ions lying out of the plane. Using an approach to reduce the complexity of the $6^{17}/6^{19}$ fold Hilbert space of the spin Hamiltonian approach, $S = 35/2$ was assigned to **Fe_{19}heidi** and $S = 25/2$ to **Fe_{17}heidi**.[34] Later magnetic characterization of a pure form of the Fe_{19} species, obtained by using a different capping organic ligand, **Fe_{19}meth**, suggested a more likely $S = 33/2$ state.[35] However, very recently the $S = 35/2$ ground state was confirmed for the latter derivative by high-field magnetization measurements and single-crystal W-band EMR spectra.[36] This technique provided interesting results, in that powder EMR spectra show no resolved fine structure, suggesting that the high number of spins induces a decisive step forward towards MNP behavior. On the other hand, the single-crystal W-band spectra partially reverse this view, because clear fine-structure components can be observed at some orientations. Furthermore the analysis, using a simple model, of the experimentally determined magnetic anisotropy of this cluster pointed out the dominant contribution of the external ions to the global anisotropy of the molecule, in analogy to the dominant contribution of surface ions in determining the magnetic anisotropy of the MNP. The compound **Fe_{19}meth** can therefore be considered an important bridge between MNM and MNP, showing the coexistence of magnetic behavior from both families.

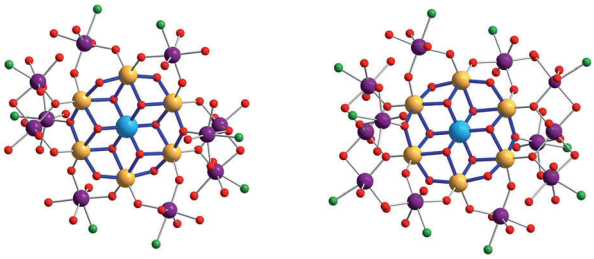

Figure 5. Structures of the **Fe_{17}heidi** and **Fe_{19}heidi** cores, occurring in the same crystal. The blue rods and the different colors of the iron centers (cyan, yellow, purple) show the brucite-type generations of the two clusters (cyan first generation, yellow second generation, purple peripheral centers).

3.3. Clusters with Non-Natural Core Structures

To conclude this survey we report some examples of clusters which demonstrates the possibility, by using suitably chosen ligands, to obtain patterns different to what is found in nature. The first example in this series is a decanuclear cage reported by Winpenny and co-workers in 1996[37a] which has an $S = 11$ ground state and was later shown to behave as an SMM at low temperature.[37b] A further example is that of an undecanuclear cluster[38] characterized by an $S = 11/2$ ground state, whose low temperature magnetic properties were interpreted assuming $D = -0.46\ cm^{-1}$ and a non-negligible rhombic anisotropy. In agreement with the easy axis anisotropy, magnetic hysteresis of molecular origin was observed. More recently a new hexadecanuclear cluster with a high spin ground state has been synthesized and preliminary characterized by DC magnetic measurements and Mossbauer spectroscopy.[39]

In addition to the cases described above, other heptadecanuclear clusters with different topology have been reported and their magnetic properties show a large variability of behaviors[10] (Table 1).

To obtain higher nuclearities, the use of polyoxometallate (POM) scaffolds has been reported to give spectacular results.[40] The most relevant system in this field is

Table 1: Relevant parameters for selected iron oxo based molecular nanomagnet.

Cluster[a]	S	V_{core}[a] [Å^3]	D [cm^{-1}]	K[b] [10^6 erg cm^{-3}]	M_S^{vol}[c] [emu cm^{-3}]	M_S[c] [μ_B/Fe]	Related oxide structures	Ref.
Fe_8Br	10	441.8	−0.2	8.96	419.98	2.5	–	[18, 19]
Fe_9heia	25/2	426.3	−0.07	5.06	542.54	2.77	Magnetite	[32]
Fe_9hpdta	13/2	475.9	−0.15	2.62	257.91	1.47	–	[57]
Fe_{10}dbm	0	418.2	–	–	–	n.r.	Lepidocrocite	[27]
Fe_{10}Mesal	0	449.7	–	–	43.3	0.21	Lepidocrocite	[28]
Fe_{10}chp	11	486.4	−0.03	1.51	400.55	2.1	–	[37ab]
Fe_{11}Bz	1/2	529.8	–	–	59.71	0.31	–	[11]
Fe_{11}thme	11/2	534.6	−0.46	5.19	187.07	0.98	–	[38]
Fe_{12}	2[d]	488.98	n.r.		141.16	0.62	–	[58]
Fe_{14}	n.r.		n.r.		–	n.r.	Hematite	[30]
Fe_{16}	15	719	0.09	2.82	386.9	1.87	–	[39]
Fe_{17}Bz	2		n.r.			0.31	–	[10a]
Fe_{17}py	35/2	718.1	−0.02	1.35	452.44	2.06	Magnetite	[32]
Fe_{17}heidi	25/2		n.r.			1.47[e]	Brucite	[33, 34]
Fe_{19}meth	35/2	948.8	−0.03	1.52	343.7	1.85	Brucite	[35, 36]
Fe_{30}	0	5634	–	–	61.7[f]	2.5[f]	–	[40]

[a] Volume of the core calculated by considering the Van der Waals volume of all the iron atoms and the atoms of their first coordination sphere. n.r. = not reported. [b] Anisotropy energy density calculated as $K = |D|\,(erg)\,S^2/V_{core}(cm^3)$. [c] Saturation magnetization obtained by measurements at the lowest reported temperature and 5 T, except when otherwise stated. [d] The ground state refers to a $Fe_4^{III}Fe_4^{II}$ subcluster, the remaining 4 Fe^{II} centers being uncoupled. [e] Estimated by the difference of the magnetization saturation data reported in Refs. [33, 34] and [35]. [f] Saturation magnetization measured at 0.5 K and 17.7 T.[40b]

undoubtedly the **Fe_{30}** molecule in which 30 Fe^{III} ions are at the vertices of the highly symmetric icosidodecahedron, mimicking an antiferromagnetic hollow sphere. This species can be considered as a zero-dimensional analogue of the planar Kagomè lattice that is composed of corner-sharing triangles arranged around hexagons. The classical Heisenberg model based on a tripartite lattice provided a good agreement with DC magnetic experimental data. In particular the linear increase of the magnetization with the field up to a saturation value was explained by considering that in zero field the vectors characterizing the three sublattices are coplanar and making an angle of 120°, while on increasing the field they tend to orient along it, becoming collinear at the saturation field.[41] The same model was however not able to explain the differential susceptibility data below 5 K and the absence of distinct quantum effects in the M versus H curve (e.g. plateau and steps) which were predicted to occur below approximately 50 mK.[41] Both these discrepancies with the simplest model have been recently rationalized by considering a two-parameters probability distribution for the 60 nearest-neighbor interactions.[42]

However, the most interesting point in the context of this Minireview is to notice that **Fe_{30}** has essentially a "dead" shell, that is, a magnetically non-ordered external layer, such as those recently found in ultra small MNP (see next Section). An investigation of **Fe_{30}** based on this approach may shed new light on the properties of MNP, similar to the way in which the recently reported results for **Fe_{19}meth** have.[36]

4. Magnetic Nanoparticles

There are very few reports on extremely small iron oxide MNP ($d < 2$ nm; Table 2).[43,44] More articles have been published on iron oxide MNP with dimension $2\text{ nm} < d < 3\text{ nm}$[45–48] (Table 2). The control of the structure of small MNP ($d < 3$ nm) is still more an art than a well established technique. Several different procedures have been proposed, including the use of thermal decomposition,[46] precipitation in constrained media,[14,45,49,50] co-precipitation,[43] polymer-based methods[51] and sol-gel.[52] Chaudret and co-workers reported a method in which, starting from the organometallic precursor $[Fe\{N(SiMe_3)_2\}_2]$ and using amines for keeping the particles well separated, reasonably monodisperse maghemite particles of approximately 2.8 nm diameter were obtained, although the average size was estimated only by magnetic measurements.[46a] Mössbauer and HRTEM were in agreement with cubic maghemite. The estimated dimensions correspond to approximately 420 iron ions for a spherical MNP.

The parameters which are more sensitive to the particle size are the saturation magnetization, M_S, and the anisotropy energy density. In a qualitative way, both depend on the ratio between surface and bulk ions, N_S. A large N_S decreases the symmetry of the particles and induces a decrease of M_S and an increase of K. Indeed, a decrease of the saturation magnetization is observed on decreasing the size of maghemite MNP (Table 2). This trend has been interpreted in terms of a core–shell model in which the arrangement of the iron ions of the core is essentially that of the bulk with a magnetically disordered external layer in which the number and symmetry of coordination of the Fe ions is different from that of the core ones. Monte Carlo simulations, based on this core–shell model,[53] correctly reproduced the observed results, indicating that already for nanoparticles of 2.5 nm, 95% of the Fe belongs to the external shell and only 17 Fe ions to the core.

Table 2: Saturation magnetization (M_S) and magnetic anisotropy (K), for iron oxide MNP of different sizes (d).

Sample	d [nm]	M_S^{vol} [emu cm^{-3}]	M_S [μ_B/atom][a]	K [10^6 erg cm^{-3}]	Ref.
γ-Fe_2O_3	2.5	142.1	0.42 (5 K)	4.7	[45]
γ-Fe_2O_3	2.8–3	53.9–115.6	0.16–0.34 (2 K)	1.26	[46a]
γ-Fe_2O_3	3.5	292.5	0.85 (1.8 K)	2.3	[14]
γ-Fe_2O_3	3.1	156.8	0.46 (2.5 K)	0.67	[15]
γ-Fe_2O_3	7	349.9	1.02 (1.8 K)	0.16	[4]
Fe_3O_4	5			0.58	[48]
Fe_3O_4	2.5			< 0.5	[48]
γ-Fe_2O_3	3.5	48.5	0.14 (5 K)		[47]
γ-Fe_2O_3	3.9	207.3	0.6 (5 K)		[47]
γ-Fe_2O_3	1.5	63.7[b]	0.19 (5 K)		[42b]
	2.2	254.8[b]	0.74 (5 K)		
	3.0	249.9[b]	0.73 (5 K)		
γ-Fe_2O_3	bulk	362.6	1.06	0.01	[59]
Fe_3O_4	bulk	459	1.24	0.01, 0.11	[59, 60]

[a] The measurement temperature is given in parentheses. [b] Data evaluated from the graphics in the original References.

The disordered layer was experimentally found to have a constant thickness of 1 nm, independent of the size of the particle.[46] Demortière et al.[45] noted that this thickness corresponds to one crystalline unit cell of γ-Fe_2O_3/Fe_3O_4 (0.834/0.839 nm)[54] and that it therefore significantly affects the properties of very small NP that may only contain a few unit cells. The thickness of this "dead" shell is in agreement with average values estimated by different techniques for bigger particles (see References in Ref. [46]). The saturation magnetization of the shell was found to be 30 emu g^{-1} compared to 91 emu g^{-1} for the core, the core value being close to the Fe_3O_4 bulk value (Table 2).[46] Similar considerations hold for the anisotropy density, K, which tends towards the bulk value on increasing d (see Table 2).

It is interesting to compare these trends with those of sufficiently large MNM, also with the goal of estimating a limiting value for the magnetic anisotropy of very small MNP, as reported in Table 1 and Figure 6. For systems with $20 > n > 16$, K increases on decreasing the number of Fe ions of the cluster: this trend roughly follows that observed for MNP. On further decreasing the size of the cluster, the relative arrangement of the iron ions plays an increasingly important role, finally reaching the limit for the single ion anisotropy in a mononuclear complex.

Another crucial point to consider is the comparison of the shell thickness of the two classes. Even if a clear identification of a magnetic surface for MNM is not obvious in most cases, **Fe_{19}meth** can provide useful insights into this aspect. As mentioned in Section 3.2, the 12 peripheral Fe^{III} ions which on the basis of the high similarity of their coordination spheres can be identified as "shell", provide a dominant contribution

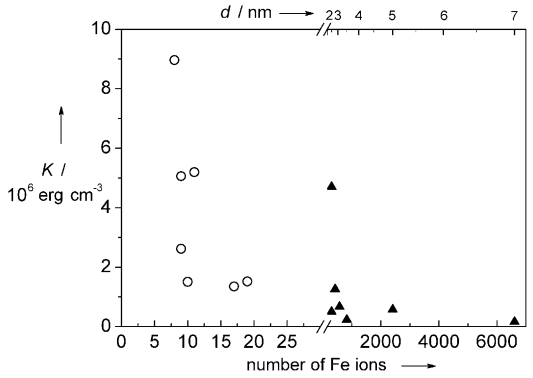

Figure 6. Trend of the anisotropy constant, obtained from literature data, on varying the dimensions for MNM (empty circles) and MNP (black triangles).

to the total anisotropy.[36] In this case it can then be considered that approximately 60% of the Fe^{III} lies on the surface and a shell thickness of 2 Å would be estimated, corresponding to the single-ion bond length. This has to be compared with MNP, for which the dead shell extends well beyond the first layer of the surface.[43] It has however to be considered that in **Fe_{19}meth** the second generation Fe^{III} ions are structurally different from a "bulk" type iron(III), since their nearest neighbors are the 12 "surface" ions. It can thus be argued that the only purely core ion in **Fe_{19}meth** is the 1st generation one (see Figure 5 for the ion generations in Fe_{19} clusters), characterized by a trigonally distorted coordination. This situation would provide a core/shell ratio of about 95%, similar to that observed for MNP. This reasoning is however purely speculative since it is based only on a single and relatively small cluster. Many more examples of larger clusters, based on the iron oxo type structures, with well characterized magnetic properties would be needed to give a definite answer to the question of "what is the shell?" in a MNM.

In addition to magnetic measurements, EMR has also been used for the characterization of MNP, even if there is not a widely accepted interpretation of the experimental spectra.[55] More recently it was shown that EMR is very sensitive to the quantum effects in small MNPs, a fact that can be completely overlooked by the magnetic characterization alone.[2–4,14]

Particularly interesting results have been obtained by the EMR investigations of maghemite/magnetite synthesized in the nano-bioreactors ferritin and LiDps[3,14] comprising approximately 4000 and 400 Fe centers, respectively. The EMR spectra of MNP mineralized in ferritin and LiDps recorded at X-band (9 GHz) have a temperature behavior very similar to that observed for the W-band (95 GHz) powder spectra of the **Fe_{19}meth** cluster (Figure 7).[4,36] The width of the main resonance increases as the temperature decreases. In MNP, this change is due to the reduced fluctuation of the magnetization as the temperature decreases, resulting in a reduced thermal averaging, such that the anisotropy field of the MNP becomes more effective in influencing the resonance position.

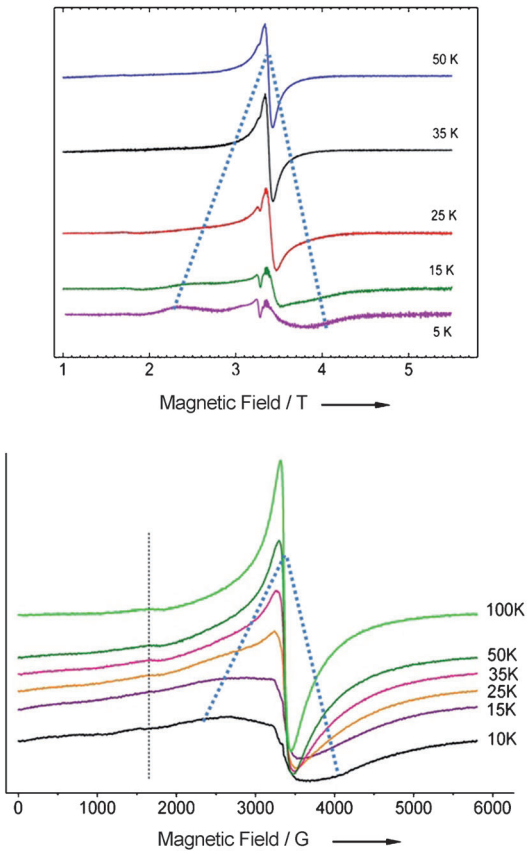

Figure 7. Comparison of the thermal behavior of the powder EMR spectra of **Fe_{19}meth** in W-band (left) and of LiDps-grown Fe_2O_3 MNP at X-band (right), showing the effect of the anisotropy (blue dashed line) on the spectrum. The vertical dotted line in X-band spectra evidences the $\Delta M = \pm 2$ transition.

Moreover, different components are present in the EMR spectra of MNP, which also have their counterpart in the **Fe_{19}meth** spectra: a signal at half-field, $B_0/2$, and a sharp line appearing at high temperature. Although the origin of this last feature is still a matter of debate for MNP, the presence of these signals has stimulated a quantum mechanics approach for the analysis of the EMR spectra of MNP, prompted also by the failure of the classical models in reproducing the experimental spectra.

When using a quantum mechanics approach, a giant spin S, determined by the exchange interaction, is associated with each particle, in analogy to the approach reported in Section 2 for molecular clusters. The spin Hamiltonian used to describe the MNP EMR spectra then contains both Zeeman and zero field splitting (ZFS) interactions, relative to the giant spin. As a result of the predominant surface contribution to the anisotropy, the ZFS term can be considered axial for very small MNP. In this framework, the appearance of a $B_0/2$ signal is attributed to the non-coincidence, as it occurs in powder samples, between the external field ($\boldsymbol{B_0}$ in the Zeeman term) and the easy axis direction (ZFS term), that is, the quantization axis being at an intermediate orientation between the two. This generates admixing between adjacent M states which results in the observation of a signal occurring at $B_0/2$,

arising from otherwise forbidden transitions $M \rightarrow M+2$. This result shows the discrete character of energy levels and therefore the quantum nature of these systems.

An important parameter which influences the relative intensity of the resonances at B_0 and $B_0/2$ is the ratio between the ZFS and Zeeman terms, which dictates the intensity of the different features in the EMR spectra. This value is accidentally similar for MNP, mineralized in LiDps and ferritin, investigated at X-band, and **Fe_{19}meth** investigated at W-band. This coincidence makes a direct comparison of the two systems particularly suited.[4]

The giant spin model has however to be used keeping in mind its limitations, the principal one being that of neglecting low-lying excited spin multiplets. Using the knowledge and recent findings on SMM, we recognize that most of the temperature behavior of EMR spectra of MNP has to be attributed to the contribution of excited *S* states and not only to the population of M-levels lying at higher energies within the S ground state.

On increasing the temperature, not only excited states get populated, but also the effect of the exchange may change. In a first approximation, the surface of the MNP can be regarded as a two-dimensional magnetic lattice with respect to the exchange interaction, instead of the three-dimensional lattice of the core ions. On decreasing the MNP size, this two-dimensional magnetic lattice will play an increasingly pronounced role, weakening the exchange interaction, such that it is reasonable to assume that at high temperature, core and surface spins will be effectively independent of each other.

5. Conclusions

Herein we have shown, through few representative examples, how the comparison of the structural and magnetic properties of MNM and MNP can be instructive for gaining a deeper understanding of the magnetic behavior at the intermediate scale between molecular and bulk objects.

In particular, we tried to develop a common ground by directly comparing the most relevant magnetic features of the two classes, by expressing the relevant physical quantities in the same units, and applying the same concepts to both classes. Thus, the study of increasingly large molecular clusters may provide valuable information to model the development of surface anisotropy and of a spin dead layer, which are critical points to explain the behavior of very small MNP.

Nevertheless, even if the size of the two classes of systems is merging, we believe that this Minireview clearly shows that there is still a significant gap, owing to the large differences in the actual number of interacting magnetic ions (30 for MNM and ca. 400 for MNP). Therefore a major synthetic effort is required to synthesize very small uniform iron oxide MNP (<1.5 nm) and molecular clusters comprising a much larger number of oxo-bridged Fe ions than have been prepared to date. Furthermore, it is striking to find that, despite two decades of efforts in the synthesis of large iron oxo based molecular cluster by many inorganic chemists,[56] the number of such systems which have their magnetic properties thoroughly characterized in terms of ground state, saturation magnetization, and anisotropy (magnitude and orientation), can be counted on the fingers of two hands. This lack of detailed information means the recognition of trends and extrapolation toward MNP behavior is still based essentially on qualitative considerations. We feel that an effort in this direction might produce relevant results for our understanding of the emergence of MNP properties from MNM ones and vice versa.

Received: August 1, 2011
Revised: January 13, 2012
Published online: April 4, 2012

[1] a) T. Hyeon, *Chem. Commun.* **2003**, 927; b) *Nanomagnetism and Spintronics* (Ed.: T. Shinjo), Elsevier, Amsterdam, **2009**; c) *Magnetism in Medicine: A Handbook* (Eds.: W. Andra, H. Nowak), Wiley-VCH, Weinheim, **2007**; d) A. K. Gupta, M. Gupta, *Biomaterials* **2005**, *26*, 3995; e) Q. A. Pankhurst, J. Connolly, S. K. Jones, J. Dobson, *J. Phys. D* **2003**, *36*, R167.

[2] N. Noginova, T. Weaver, E. P. Giannelis, A. B. Bourlinos, V. A. Atsarkin, V. V. Demidov, *Phys. Rev. B* **2008**, *77*, 014403.

[3] H. Li, M. T. Klem, K. B. Sebby, D. J. Singel, M. Young, T. Douglas, Y. U. Idzerda, *J. Magn. Magn. Mater.* **2009**, *321*, 175.

[4] M. Fittipaldi, C. Innocenti, P. Ceci, C. Sangregorio, L. Castelli, L. Sorace, D. Gatteschi, *Phys. Rev. B* **2011**, *83*, 104409.

[5] J. Tejada, X. X. Zhang, E. delBarco, J. M. Hernandez, E. M. Chudnovsky, *Phys. Rev. Lett.* **1997**, *79*, 1754.

[6] a) A. Caneschi, D. Gatteschi, R. Sessoli, A. L. Barra, L. C. Brunel, M. Guillot, *J. Am. Chem. Soc.* **1991**, *113*, 5873; b) R. Sessoli, D. Gatteschi, A. Caneschi, M. A. Novak, *Nature* **1993**, *365*, 141.

[7] a) L. Thomas, F. Lionti, R. Ballou, D. Gatteschi, R. Sessoli, B. Barbara, *Nature* **1996**, *383*, 145; b) J. R. Friedman, M. P. Sarachik, J. Tejada, R. Ziolo, *Phys. Rev. Lett.* **1996**, *76*, 3830.

[8] R. Sessoli, J. Villain, D. Gatteschi, *Molecular Nanomagnets*, Oxford University Press, Oxford, **2006**.

[9] a) "Metal Sites in Proteins and Models": A. K. Powell in *Structure and Bonding*, *Vol. 88* (Eds.: H. A. O. Hill, P. J. Sadler, A. J. Thomson), Springer, Berlin, **1997**, S. 1; b) D. J. Price, F. Lionti, R. Ballou, P. T. Wood, A. K. Powell, *Philos. Trans. R. Soc. London Ser. A* **1999**, *357*, 3099; c) K. L. Taft, G. C. Papaefthymiou, S. J. Lippard, *Science* **1993**, *259*, 1302.

[10] a) W. Micklitz, V. McKee, R. Lynn Rardin, L. E. Pence, G. C. Papaefthymiou, S. G. Both, S. J. Lippard, *J. Am. Chem. Soc.* **1994**, *116*, 8061; b) S. Parsons, G. A. Solan, R. E. P. Winpenny, *J. Chem. Soc. Chem. Commun.* **1995**, 1987.

[11] S. M. Gorun, G. C. Papaefthymiou, R. B. Frankel, S. J. Lippard, *J. Am. Chem. Soc.* **1987**, *109*, 3337.

[12] M. Fittipaldi, L. Sorace, A. L. Barra, C. Sangregorio, R. Sessoli, D. Gatteschi, *Phys. Chem. Chem. Phys.* **2009**, *11*, 6555.

[13] E. Chiancone, P. Ceci, A. Ilari, F. Ribacchi, S. Stefanini, *Biometals* **2004**, *17*, 197.

[14] P. Ceci, E. Chiancone, O. Kasyutich, G. Bellapadrona, L. Castelli, M. Fittipaldi, D. Gatteschi, C. Innocenti, C. Sangregorio, *Chem. Eur. J.* **2010**, *16*, 709.

[15] M. Uchida, M. T. Klem, M. Allen, P. Suci, M. Flenniken, E. Gillitzer, Z. Varpness, L. O. Liepold, M. Young, T. Douglas, *Adv. Mater.* **2007**, *19*, 1025.

[16] A. H. Morrish, *The Physical Principles of Magnetism*, Wiley-Interscience, New York, **1962**.

[17] The volumes of MNP were estimated by their average diameter while for MNM the volume of the van der Waals surface of the core (i.e. iron centers and the atoms of their first coordination

sphere) was calculated using Discovery Studio 3.0. see: http://www.accelrys.com/products/discovery-studio/.
[18] A. L. Barra, P. Debrunner, D. Gatteschi, C. E. Schulz, R. Sessoli, *Europhys. Lett.* **1996**, *35*, 133.
[19] a) C. Sangregorio, T. Ohm, C. Paulsen, R. Sessoli, D. Gatteschi, *Phys. Rev. Lett.* **1997**, *78*, 4645; b) W. Wernsdorfer, R. Sessoli, *Science* **1999**, *284*, 133.
[20] K. Wieghardt, K. Pohl, I. Jibril, J. Huttner, *Angew. Chem.* **1984**, *96*, 66; *Angew. Chem. Int. Ed. Engl.* **1984**, *23*, 77.
[21] a) A. L. Barra, D. Gatteschi, R. Sessoli, *Chem. Eur. J.* **2000**, *6*, 1608; b) R. Caciuffo, G. Amoretti, A. Murani, R. Sessoli, A. Caneschi, D. Gatteschi, *Phys. Rev. Lett.* **1998**, *81*, 4744.
[22] a) A. L. Barra, A. Caneschi, A. Cornia, D. Gatteschi, L. Gorini, L. P. Heiniger, R. Sessoli, L. Sorace, *J. Am. Chem. Soc.* **2007**, *129*, 10754; b) E. Liviotti, S. Carretta, G. Amoretti, *J. Chem. Phys.* **2002**, *117*, 3361; c) A. Wilson, J. Lawrence, E. C. Yang, M. Nakano, D. N. Hendrickson, S. Hill, *Phys. Rev. B* **2006**, *74*, 140403.
[23] K. L. Taft, C. D. Delfs, G. C. Papapefthymiou, S. Foner, D. Gatteschi, S. J. Lippard, *J. Am. Chem. Soc.* **1994**, *116*, 823.
[24] O. Waldmann, R. Koch, S. Schromm, J. Schülein, P. Müller, I. Bernt, R. W. Saalfrank, F. Hampel, E. Balthes, *Inorg. Chem.* **2001**, *40*, 2986.
[25] J. Dreiser, O. Waldmann, G. Carver, C. Dobe, H.-U. Güdel, H. Weihe, A.-L. Barra, *Inorg. Chem.* **2010**, *49*, 8729.
[26] P. Baran, R. Boča, I. Chakraborty, J. Giapintzakis, R. Herchel, Q. Huang, J. E. McGrady, R. G. Raptis, Y. Sanakis, A. Simopoulos, *Inorg. Chem.* **2008**, *47*, 645.
[27] A. Caneschi, A. Cornia, A. C. Fabretti, D. Gatteschi, *Angew. Chem.* **1995**, *107*, 2862; *Angew. Chem. Int. Ed. Engl.* **1995**, *34*, 2716.
[28] a) S. Asirvatham, M. A. Khan, K. M. Nicholas, *Inorg. Chem.* **2000**, *39*, 2006; b) T. Glaser, T. Lugger, R.-D. Hoffmann, *Eur. J. Inorg. Chem.* **2004**, 2356.
[29] M. D. Godbole, O. Roubeau, A. M. Mills, H. Kooijman, A. L. Spek, E. Bouwman, *Inorg. Chem.* **2006**, *45*, 6713.
[30] J. Burger, P. Klüfers, *Angew. Chem.* **1997**, *109*, 801; *Angew. Chem. Int. Ed. Engl.* **1997**, *36*, 776.
[31] C. Carbone, F. Di Benedetto, C. Sangregorio, P. Marescotti, L. A. Pardi, L. Sorace, *J. Phys. Chem. C* **2008**, *112*, 9988.
[32] a) G. W. Powell, H. N. Lancashire, E. K. Brechin, D. Collison, S. L. Heath, T. Mallah, W. Wernsdorfer, *Angew. Chem.* **2004**, *116*, 5896; *Angew. Chem. Int. Ed.* **2004**, *43*, 5772; b) M. Evangelisti, A. Candini, A. Ghirri, M. Affronte, G. W. Powell, I. A. Gass, P. A. Wood, S. Parsons, E. K. Brechin, D. Collison,, S. L. Heath, *Phys. Rev. Lett.* **2006**, *97*, 167202.
[33] A. K. Powell, S. L. Heath, *Angew. Chem.* **1992**, *104*, 1290; *Angew. Chem. Int. Ed. Engl.* **1992**, *31*, 930.
[34] A. K. Powell, S. L. Heath, D. Gatteschi, L. Pardi, R. Sessoli, G. Spina, F. Del Giallo, F. Pieralli, *J. Am. Chem. Soc.* **1995**, *117*, 2491.
[35] J. C. Goodwin, R. Sessoli, D. Gatteschi, W. Wernsdorfer, A. K. Powell, S. L. Heath, *J. Chem. Soc. Dalton Trans.* **2000**, 1835.
[36] L. Castelli, M. Fittipaldi, A. K. Powell, D. Gatteschi, L. Sorace, *Dalton Trans.* **2011**, *40*, 8145.
[37] a) C. Benelli, S. Parsons, G. A. Solan, R. E. P. Winpenny, *Angew. Chem.* **1996**, *108*, 1967; *Angew. Chem. Int. Ed. Engl.* **1996**, *35*, 1825; b) C. Benelli, J. Cano, Y. Journaux, R. Sessoli, G. A. Solan, R. E. P. Winpenny, *Inorg. Chem.* **2001**, *40*, 188.
[38] L. F. Jones, E. K. Brechin, D. Collison, M. Helliwell, T. Mallah, S. Piligkos, G. Rajaraman, W. Wernsdorfer, *Inorg. Chem.* **2003**, *42*, 6601.
[39] A. M. Ako, V. Mereacre, Y. Lan, C. E. Anson, A. K. Powell, *Chem. Eur. J.* **2011**, *17*, 4366.
[40] a) A. Müller, S. Sarkar, S. Q. N. Shah, H. Bögge, M. Schmidtmann, S. Sarkar, P. Kögerler, B. Hauptfleisch, A. Trautwein, V. Schünemann, *Angew. Chem.* **1999**, *111*, 3435; *Angew. Chem. Int. Ed.* **1999**, *38*, 3238; b) A. Müller, M. Luban, C. Schröder, R. Modler, P. Kögerler, M. Axenovich, J. Schnack, P. C. Canfield, S. Bud'ko, N. Harrison, *ChemPhysChem* **2001**, *2*, 517.
[41] C. Schröder, H. Nojiri, J. Schnack, P. Hage, M. Luban, P. Kögerler, *Phys. Rev. Lett.* **2005**, *94*, 017205.
[42] C. Schröder, R. Prozorov, P. Kögerler, M. D. Vannette, X. Fang, M. Luban, A. Matsuo, K. Kindo, A. Müller, A. M. Todea, *Phys. Rev. B* **2008**, *77*, 224409.
[43] A. Millan, A. Urtizberea, N. J. O. Silva, F. Palacio, V. S. Amaral, E. Snoeck, V. Serin, *J. Magn. Magn. Mater.* **2007**, *312*, L5.
[44] D. Bonacchi, A. Caneschi, D. Dorignac, A. Falqui, D. Gatteschi, D. Rovai, C. Sangregorio, R. Sessoli, *Chem. Mater.* **2004**, *16*, 2016.
[45] A. Demortière, P. Panissod, B. P. Pichon, G. Pourroy, D. Guillon, B. Donnio, S. Begin-Colin, *Nanoscale* **2011**, *3*, 225.
[46] a) A. Glaria, M. L. Kahn, A. Falqui, P. Lecante, V. Colliere, M. Respaud, B. Chaudret, *ChemPhysChem* **2008**, *9*, 2035; b) B. H. Kim, N. Lee, H. Kim, K. An, Y. I. Park, Y. Choi, K. Shin, Y. Lee, S. G. Kwon, H. B. Na, J.-G. Park, T.-Y. Ahn, Y.-W. Kim, W. K. Moon, S. H. Choi, T. Hyeon, *J. Am. Chem. Soc.* **2011**, *133*, 12624.
[47] M. P. Morales, M. Andres-Verges, S. Veintemillas-Verdaguer, M. I. Montero, C. J. Serna, *J. Magn. Magn. Mater.* **1999**, *203*, 146.
[48] J. M. Vargas, E. Lima, R. D. Zysler, J. G. S. Duque, E. de Biasi, M. Knobel, *Eur. Phys. J. B* **2008**, *64*, 211.
[49] K. Gilmore, Y. U. Idzerda, M. T. Klem, M. Allen, T. Douglas, M. Young, *J. Appl. Phys.* **2005**, *97*, 10B301.
[50] a) N. Feltin, M. P. Pileni, *Langmuir* **1997**, *13*, 3927; b) Y. Lee, J. Lee, C. J. Bae, J.-G. Park, H.-J. Noh, J.-H. Park, T. Hyeon, *Adv. Funct. Mater.* **2005**, *15*, 503.
[51] J. Ramos, A. Millan, F. Palacio, *Polymer* **2000**, *41*, 8461.
[52] C. Cannas, G. Concas, D. Gatteschi, A. Musinu, G. Piccaluga, C. Sangregorio, *J. Mater. Chem.* **2002**, *12*, 3141.
[53] O. Iglesias, A. Labarta, *Phys. Rev. B* **2001**, *63*, 184416.
[54] *International Center for Diffraction Data*: magnetite JPCDS 19-0629; maghemite JPCDS 39-1346.
[55] a) Y. L. Raikher, V. I. Stepanov, *Sov. Phys. JETP* **1992**, *75*, 764; b) J. Kliava, R. Berger, *J. Magn. Magn. Mater.* **1999**, *205*, 328; c) N. Noginova, F. Chen, T. Weaver, E. P. Giannelis, A. B. Bourlinos, V. A. Atsarkin, *J. Phys. Condens. Matter* **2007**, *19*, 246208.
[56] a) T. Taguchi, M. S. Thompson, K. A. Abboud, G. Christou, *Dalton Trans.* **2010**, *39*, 9131; b) R. Bagai, K. A. Abboud, G. Christou, *Chem. Commun.* **2007**, 3359; c) D. Foguet-Albiol, K. A. Abboud, G. Christou, *Chem. Commun.* **2005**, 4282; d) W. Schmitt, L. Zhang, C. E. Anson, A. K. Powell, *Dalton Trans.* **2010**, *39*, 10279; e) I. A. Gass, C. J. Milios, A. Collins, F. J. White, L. Budd, S. Parsons, M. Murrie, S. P. Perlepes E. K. Brechin, *Dalton Trans.* **2008**, 2043.
[57] W. Schmitt, C. E. Anson, W. Wernsdorfer, A. K. Powell, *Chem. Commun.* **2005**, 2098.
[58] A. Caneschi, A. Cornia, S. J. Lippard, G. C. Papaefthymiou, R. Sessoli, *Inorg. Chim. Acta* **1996**, *243*, 295.
[59] R. M. Cornell, U. Schwertmann, *The Iron Oxides*, Wiley-VCH, Weinheim, **1996**.
[60] M. Schieber, *Experimental Magnetochemistry: Non-Metallic Magnetic Materials*, North-Holland, Amsterdam, **1967**.